Gas-Phase Electron Transfer: Thermal Self-Exchange and Cross Reactions of Organometallic Molecules and Ions

David E. Richardson,* Charles S. Christ, Paul Sharpe, and John R. Eyler*

Contribution from the Department of Chemistry, University of Florida, Gainesville, Florida 32611. *Received October 27, 1986*

Abstract: Fourier transform ion cyclotron resonance has been used to investigate electron-transfer reactions in the gas phase. The rate constants for thermal electron-transfer reactions are given for 10 self-exchange reactions and 11 cross reactions involving primarily metallocene and metallocenium reactants. The advantages of using ion intensity ratios to determine the rate constants are described. For reactions with low exoergicities, the estimated inner reorganizational barriers correlate with the observed efficiencies. Many of the rate constants approach the collisional maximum since small reorganization of bond distances is required, and inefficient reactions are associated with large changes in bond distances or bond angles. Among the metallocenes, inefficient self-exchange and cross reactions are associated with the manganocenes, which have a high-spin/low-spin equilibrium in the neutral form; the rates of the self-exchange reactions decrease for increasing high-spin character ($Cp_2Mn^{+/0}$, $k_f = 1.3 \times 10^{-11}$ cm^3 s^{-1}; $(MeCp)_2Mn^{+/0}$, $k_f = 4.2 \times 10^{-11}$ cm^3 s^{-1}; $(Me_5Cp)_2Mn^{+/0}$, $k_f = 3 \times 10^{-10}$ cm^3 s^{-1}). All rate constants for Cp_2Ru^+/Cp_2M and $Cp_2Ru^+/(Me_5Cp)_2M$ cross reactions (driving force $\Delta E°$ from −0.6 to −2.8 eV) are close to the Langevin rate constant ($1.0 \pm 0.5 \times 10^{-9}$ cm^3 s^{-1}). Therefore, no "inverted" region is observed, and reasons for its absence are discussed. In particular, the estimated Franck–Condon factors deduced from photoelectron spectroscopy can be used to rationalize the efficiencies of the electron-transfer reactions. For the metallocenes where adequate structural and vibrational data are available, the calculated Franck–Condon factors for ion–neutral interconversions significantly underestimate the observed widths in the photoelectron spectra. Possible contributions to the Franck–Condon widths not incorporated into the simple treatment are considered.

Intermolecular and intramolecular electron-transfer reactions in condensed phases[1-10] have not traditionally been considered in the same context as gas-phase electron-transfer reactions[11-36] despite the clear similarity of the phenomena. A survey of the literature reveals only a minimal amount of cross-referencing between the two subjects. Condensed-phase electron-transfer processes were first systematized theoretically more than three decades ago;[1,2] in many cases, the theoretical models can predict the rates of electron-transfer reactions within an order of magnitude.[1,5] Currently, topics such as solvent dynamics[6,7] and weak electronic interactions[8-10] are areas of intense interest. Electron-transfer reactions are an important class of gas-phase reactions which have been studied extensively.[11-24] Since small reactants (atomic or diatomic) are typically studied and no solvent is involved, complete quantum mechanical treatments have been developed which are largely successful in predicting overall reactive cross sections.[26-28] Although thermal reactions have been investigated,[12,15,19,21-23,25] experimental and theoretical studies have largely involved collisions of accelerated ions with thermal neutrals. The study of kinetics of ion/molecule electron transfer has often been associated with the development of charge-transfer chemical ionization mass spectrometry (CT-CI).[16,29-31]

The general picture which emerges is one of two experimentally and theoretically well-developed areas involving gas-phase electron-transfer reactions of small reactants on the one hand and condensed-phase electron-transfer reactions of large, often metal-containing, reactants on the other. The kinetics and theoretical

(1) For recent reviews, see: (a) Marcus, R. A.; Sutin, N. *Biochim. Biophys. Acta* **1985**, *811*, 265. (b) Sutin, N. *Prog. Inorg. Chem.* **1983**, *30*, 441. (c) Sutin, N. *Acc. Chem. Res.* **1982**, *15*, 275–82. (d) Newton, M. D.; Sutin, N. *Annu. Rev. Phys. Chem.* **1984**, *35*, 437.

(2) (a) Cannon, R. D. *Electron-Transfer Reactions*; Butterworths: London, 1980. (b) Ulstrup, J. *Charge-Transfer Processes in Condensed Media*; Springer-Verlag: West Berlin, 1979.

(3) (a) Kestner, N. R.; Logan, J.; Jortner, J. *J. Phys. Chem.* **1974**, *78*, 2148. (b) Van Duyne, R.; Fischer, S. *Chem. Phys.* **1974**, *5*, 183. (c) Ulstrup, J.; Jortner, J. *J. Chem. Phys.* **1975**, *63*, 4358. (d) Onuchic, J. N.; Beratan, D. N.; Hopfield, J. J. *J. Phys. Chem.* **1986**, *90*, 3707.

(4) (a) Brunschwig, B. S.; Logan, J.; Newton, M. D.; Sutin, N. *J. Am. Chem. Soc.* **1980**, *102*, 5798. (b) Scher, H.; Holstein, T. *Philos. Mag.*, [*Part*] *B* **1981**, *44*, 343.

(5) Brunschwig, B. S.; Creutz, C.; Macartney, D. H.; Sham, T. K.; Sutin, N. *Faraday Discuss. Chem. Soc.* **1982**, *74*, 113.

(6) See: Gennett, T.; Milner, D. F.; Weaver, M. J. *J. Phys. Chem.* **1985**, *89*, 2787 and references cited therein.

(7) Brunschwig, B. S.; Ehrenson, S.; Sutin, N. *J. Phys. Chem.* **1986**, *90*, 3657.

(8) Closs, G. L.; Calcaterra, L. T.; Green, N. J.; Penfield, K. W.; Miller, J. R. *J. Phys. Chem.* **1986**, *90*, 3673.

(9) Miller, J. R.; Beitz, J. U.; Huddleston, R. K. *J. Am. Chem. Soc.* **1984**, *106*, 5057.

(10) Mayo, S. L.; Ellis, W. R.; Crutchley, R. J.; Gray, H. B. *Science (Washington, DC)* **1986**, *233*, 948.

(11) Marx, R. In *Ionic Processes in the Gas Phase*; Almoster Ferreira, M. A., Ed.; D. Reidel: Dordrecht, Holland, 1984; pp 67–86.

(12) Turner-Smith, A. R.; Green, J. M.; Webb, C. E. *J. Phys. B* **1973**, *6*, 114.

(13) Rapp, D.; Francis, W. E. *J. Chem. Phys.* **1962**, *37*, 2631.

(14) (a) Liao, C.-L.; Shao, J.-D.; Xu, R.; Flesch, G. D.; Li, Y.-G.; Ng, C. Y. *J. Chem. Phys.* **1986**, *85*, 3874 and references cited therein. (b) Lee, C.-Y.; De Pristo, A. E.; Liao, C.-L.; Liao, C.-X.; Ng, C. Y. *Chem. Phys. Lett.* **1985**, *116*, 534. (c) Lee, C.-Y.; De Pristo, A. E. *J. Am. Chem. Soc.* **1983**, *105*, 6775 and references therein.

(15) Smith, D. L.; Futrell, J. H. *J. Chem. Phys.* **1973**, *59*, 463.

(16) Baer, T. In *Mass Spectrometry*; Specialist Periodical Report; The Chemical Society: London, 1981; Vol. 6 and earlier reviews in same series.

(17) (a) Cole, S. K.; Baer, T.; Guyon, P. M.; Govers, T. R. *Chem. Phys. Lett.* **1984**, *109*, 285. (b) Baer, T.; Murray, P. T. *J. Chem. Phys.* **1981**, *75*, 4477. (c) Baer, T.; Murray, P. T.; Squires, L. *J. Chem. Phys.* **1978**, *68*, 4901.

(18) Gurnee, E. F.; Magee, J. L. *J. Chem. Phys.* **1957**, *26*, 1237.

(19) Gauglhofer, J.; Kevan, L. *Chem. Phys. Lett.* **1972**, *16*, 492.

(20) (a) Shields, G. C.; Moran, T. F. *J. Phys. Chem.* **1985**, *89*, 4027. (b) Moran, T. F.; McCann, K. J.; Cobb, M.; Borkman, R. F.; Flannery, M. R. *J. Chem. Phys.* **1981**, *74*, 2325. (c) Flannery, M. R.; Cosby, P. C.; Moran, T. F. *J. Chem. Phys.* **1973**, *59*, 5494. (d) Leventhal, J.; Moran, T. F.; Friedman, L. *J. Chem. Phys.* **1967**, *46*, 4666.

(21) (a) Bowers, M. T.; Elleman, D. D. *Chem. Phys. Lett.* **1972**, *16*, 486. (b) Laudenslager, J. B.; Huntress, W. T.; Bowers, M. T. *J. Chem. Phys.* **1974**, *61*, 4600.

(22) McMahon, T.; Miasek, P. G.; Beauchamp, J. L. *Int. J. Mass Spectrom. Ion Phys.* **1976**, *21*, 63–71.

(23) Ausloos, P.; Eyler, J. R.; Lias, S. G. *Chem. Phys. Lett.* **1975**, *30*, 21.

(24) Turner, T.; Lee, Y. T. *J. Chem. Phys.* **1984**, *81*, 5638.

(25) (a) Mauclaire, G.; Derai, R.; Fenistein, S.; Marx, R.; Johnson, R. *J. Chem. Phys.* **1979**, *70*, 4023. (b) Mauclaire, G.; Derai, R.; Fenistein, S.; Marx, R. *J. Chem. Phys.* **1979**, *70*, 4017.

(26) Weglein, A.; Rapp, D. In *Gas Phase Ion Chemistry*; Bowers, M. T., Ed.; Academic: New York, 1979; Vol. 2, p 84.

(27) (a) Bates, D. R.; Lynn, N. *Proc. R. Soc. A* **1959**, *253*, 141. (b) Bates, D. R.; McCarroll, R. *Philos. Mag. Suppl.* **1962**, *11*, 39. (c) Bates, D. R.; Reid, R. H. G. *Proc. R. Soc. A* **1969**, *310*, 1. (d) Crothers, D. S. F. *Adv. At. Mol. Phys.* **1981**, *17*, 55.

(28) The cross section is commonly encountered in the gas phase literature and is defined as $Q = k/v_{rel}$, where k is the second-order rate constant and v_{rel} is the relative velocity of the reacting ion and molecule.

(29) Harrison, A. *Chemical Ionization Mass Spectrometry*; CRC: Boca Raton, 1983.

(30) Jowko, A.; Forys, M.; Jonsson, B. *Int. J. Mass Spectrom. Ion Phys.* **1979**, *29*, 249.

(31) Tedder, J. M.; Vidaud, P. H. *Chem. Phys. Lett.* **1979**, *64*, 81.

0002-7863/87/1509-3894$01.50/0

treatment of gas-phase electron-transfer reactions of large molecules (e.g., greater than five atoms) remain largely unexplored. Our recent work has concentrated on the development of experimental and theoretical approaches to this little-studied class of ion/molecule reactions.[32,33] In principle, the study of intrinsic barriers in gas-phase electron-transfer reactions can provide a more complete understanding of analogous reactions in solution, especially when direct comparisons can be made.

We reported a direct comparison of electron-transfer rates in gas phase and solution in our study[32] of the rate constant of ferrocene/ferrocenium self-exchange reaction measured by ion cyclotron resonance. The rate of the gas-phase reaction is close to the collisional limit, making the exchange $\gtrsim 10^4$ times faster in the absence of solvent. Any intrinsic barriers to the gas-phase electron exchange are apparently small in the case of ferrocene/ferrocenium and a number of other metallocene self-exchange reactions.[32,33] In other cases, kinetic barriers lead to inefficient gas-phase electron transfer for polyatomic organometallic,[32] nonmetal,[34,35] and organic reactants.[36] We have explained the observations of slow gas-phase electron transfer made by us and others by an adaptation of Marcus theory to ion/molecule reactions.[33] Originally developed for solution outer-sphere electron transfer,[37,38] Marcus theory has several components which translate to the gas-phase reactions considered. For reactions with significant intrinsic reorganizational barriers and zero or relatively low exoergicity, we believe that the classical Marcus theory provides a suitable "zero-order" picture of the potential barriers which tend to retard electron-transfer rates in inefficient gas-phase reactions of polyatomic reactants.

A major unresolved question in electron transfer concerns the dependence of rate on the exoergicity of the reaction. Marcus predicted some time ago[39] that under certain conditions the rate constants of homogeneous electron-transfer reactions should increase with increasingly negative $\Delta G°$ but eventually decrease (invert) once the $\Delta G°$ goes beyond a value determined by the sum of the inner and outer reorganization energies. Marcus and Siders[40] surveyed the available data in 1982 and found no strong evidence for the inverted region in a variety of experimental approaches published up to that time. Experiments involving intramolecular processes[41] and geminate radical pairs[42] have demonstrated an inverted region; however, the presence of an inverted region for bimolecular reactions is still controversial. Possible reasons for the lack of a rate effect even in favorable cases have been widely discused[3c,40,43] but not directly demonstrated.

We report here the rates of a number of electron self-exchange and cross reactions involving primarily organometallic reactants. The kinetics of these reactions are considered in light of theoretical models, and, in particular, cross reactions with high exoergicity are discussed. The results for the latter reactions have provided new insights into the questions surrounding the predicted inverted region in electron-transfer kinetics.

Experimental Section

All kinetic data were acquired with a Nicolet FT/MS-1000 Fourier transform mass spectrometer.[44] A double-resonance technique described previously[32] was employed to obtain data for the pseudo-first-order reactions. Electron impact at 10–13 eV was used for ionization. Typical pressures during the reactions ranged from 10^{-7} to 10^{-6} torr. Pressures were measured at an ionization gauge and corrected from calibration comparisons with a Baratron capacitance manometer at pressures $>10^{-5}$ torr. System pumping speed was maintained at a level which allows essentially complete pressure equilibration between the ion trap and pressure gauges on the system.

Ion signal vs. time data were recorded over a suitable time period from 3 ms initially to a final reaction time between 500 and 1000 ms. Equation 1 was used to determine second-order rate constants for self-exchange reactions and irreversible cross reactions. For self-exchange

$$\ln\left(\frac{R_t - (f'_0/f_0)}{R_t + 1}\right) = -kPt \tag{1}$$

reactions, f_0 and f'_0 are the fractional natural abundances of the ejected and nonejected isotopes respectively ($f_0 = 1 - f'_0$). R_t is the value of f'/f detected at time t after the ejection, and P is the total neutral reactant pressure. For irreversible cross reactions ($A^+ \rightarrow B^+$), f'_0/f_0 is zero and the equation simplifies to eq 2. The cross reaction between manganocene

$$\ln\left(\frac{R_t}{R_t + 1}\right) = -k_f Pt \tag{2}$$

and nickelocene established an equilibrium that was measurable directly (eq 3, Cp ≡ cyclopentadienyl). A kinetic treatment for the general case

$$Cp_2Ni^+ + Cp_2Mn \underset{k_r}{\overset{k_f}{\rightleftharpoons}} Cp_2Ni + Cp_2Mn^+ \tag{3}$$

$$A^+ \underset{k_{-1}}{\overset{k_1}{\rightleftharpoons}} B^+ \tag{4}$$

of eq 4 was therefore applicable. Here, k_1 and k_{-1} are the pseudo-first-order rate constants for the forward and reverse reactions as given in eq 5. The ratio (R_t) of the concentrations of A^+ and B^+ at time t is

$$k_1 = k_f[B] \qquad k_{-1} = k_r[A] \tag{5}$$

given by eq 6, where $k_{obsd} = (k_1 + k_{-1})$. The apparent equilibrium

$$R_t = \frac{[A^+]_t}{[B^+]_t} = \frac{k_{-1} + k_1 \exp(-k_{obsd}t)}{k_1 - k_1 \exp(-k_{obsd}t)} \tag{6}$$

constant (K_{app}) is measured from the ratio of reactant and product ion peak areas at the end of the reaction (eq 7). Substituting into eq 6 gives

$$K_{app} = \frac{[B^+]}{[A^+]} = \frac{k_1}{k_{-1}} \tag{7}$$

eq 8. From the experimental values of k_{obsd} and K_{app}, values for k_1 and k_{-1} are obtained, and these values together with eq 5 yield values for the second-order rate constants for the forward and reverse reaction, k_f and k_r.

$$\ln\left(\frac{R_t - (1/K_{app})}{1 + R_t}\right) = -k_{obsd}t \tag{8}$$

Dimethylmanganocene and decamethylcobaltocene were synthesized according to literature preparations.[45] All other metallocenes and compounds were obtained from commercial sources. Additional purification of metallocenes was achieved through vacuum sublimation, and purity was determined by mass spectral analysis.

Results

Reaction Conditions. A major concern in ion/molecule reactions is the production of "hot" or nonthermal ions. Production of hot ions may cause irreproducibility in the detected ion population and alter the efficiencies of reactions that proceed at less than the collision rate. Whether the efficiency of a reaction increases or decreases with hot ions in comparison to thermal ions depends on the sign of the temperature dependence, which can be positive

(32) Eyler, J. R.; Richardson, D. E. *J. Am. Chem. Soc.* **1985**, *107*, 6130.
(33) Richardson, D. E. *J. Phys. Chem.* **1986**, *90*, 3697.
(34) (a) Grumsrud, E. P.; Chowdhury, S.; Kebarle, P. *J. Chem. Phys.* **1985**, *83*, 1059–1068. (b) Chowdhury, S.; Kebarle, P. *J. Chem. Phys.* **1986**, *85*, 4989.
(35) Grimsrud, E. P.; Caldwell, G.; Chowdhury, S.; Kebarle, P. *J. Am. Chem. Soc.* **1985**, *107*, 4627.
(36) (a) Mautner, M.; Nelson, S. F.; Willi, M. R.; Frigo, T. B. *J. Am. Chem. Soc.* **1984**, *106*, 7384–7389. (b) Mautner, M.; Rumack D.; Nelson, S. *Abstract 338*, 10th International Mass Spectrometry Conference, Swansea, U.K., 1985.
(37) Marcus, R. A. *J. Chem. Phys.* **1956**, *24*, 966.
(38) Marcus, R. A. *Annu. Rev. Phys. Chem.* **1964**, *15*, 155.
(39) Marcus, R. A. *Discuss. Faraday Soc.* **1960**, *29*, 21.
(40) (a) Siders, P.; Marcus, R. A. *J. Am. Chem. Soc.* **1981**, *103*, 748. (b) Marcus, R. A.; Siders, P. *J. Phys. Chem.* **1982**, *86*, 622.
(41) (a) Miller, J. R.; Calcaterra, L. T.; Closs, G. L. *J. Am. Chem. Soc.* **1984**, *106*, 3047. (b) Wasielewski, M. R.; Niemczyk, M. P.; Svec, W. A.; Pewitt, E. B. *J. Am. Chem. Soc.* **1985**, *107*, 1080.
(42) Ohno, T.; Yoshimura, A.; Mataga, N. *J. Phys. Chem.* **1986**, *90*, 3295.
(43) Meyer, T. J. *Prog. Inorg. Chem.* **1983**, *30*, 441.
(44) For recent reviews of the ion cyclotron resonance technique, see: (a) Marshall, A. G. *Acc. Chem. Res.* **1985**, *18*, 316. (b) Wanczek, K. P. *Int. J. Mass Spec. Ion Proc.* **1984**, *60*, 11. (c) Gross, M. L.; Rempel, D. L. *Science (Washington, DC)* **1984**, *226*, 261.
(45) (a) Reynolds, L. T.; Wilkinson, G. *J. Inorg. Nucl. Chem.* **1959**, *9*, 86. (b) Robbins, J. L.; Edelstein, N.; Spencer, B.; Smart, J. C. *J. Am. Chem. Soc.* **1982**, *104*, 1882.

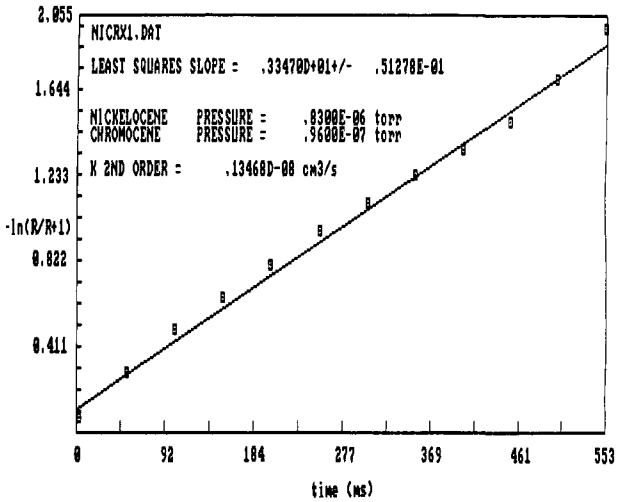

Figure 1. Typical kinetic data for an irreversible metallocene cross reaction (Cp_2Cr/Cp_2Ni^+) plotted according to eq 2. The pressures of the neutrals in the experiment (measured at an ion gauge) are indicated on the plot. The second-order rate constant, k_f, is calculated after correction of the ion gauge reading by a pressure calibration factor.

or negative. In order to minimize error in the determination of rate constants, several precautions were taken as described below.

Ions were produced by electron impact with an electron beam voltage adjusted to minimize fragmentation of the neutrals and maximize parent ion yields. Voltages were kept in the 10–13-eV range to minimize excess internal energy in the ions and to prevent the ionization of the argon buffer gas.

Since thermalization is achieved through collisions of the ions with neutrals and buffer gas, total pressures were set such that the thermalization rate was rapid compared to the reaction rate. Pressures for self-exchange reactions were adjusted in order to follow the reaction over at least 500 ms, and argon buffer gas was added usually to a pressure of about 1×10^{-6} torr. A delay time of 500 ms was instituted in the self-exchange reactions between electron impact and the ejection of the main parent ion isotope. This delay time allowed for many collisions and thus expedited thermalization before data acquisition.

Pressures for neutrals used in cross reaction studies were also adjusted to follow the reaction over at least 500 ms. In this case, the pressure of the neutral of lower ionization potential determined the time scale for the reaction. The pressure of the other neutral was then elevated to maximize the signal-to-noise ratio and to aid in thermalization. Argon buffer gas was added, and the rates were compared to reactions run with no buffer gas in order to determine the effectiveness of the neutrals in thermalization. In all cross reactions, addition of buffer gas had no significant effect on the slope or linearity of the kinetic plot. A delay of approximately 100 ms was used before ejection, and only data acquired after 200 ms of reaction were used in the calculation of the rate constant. Typical kinetic plots based on eq 1 and 8 were linear over 1.5–3 half-lives. An example of data for the Cp_2Ni^+/Cp_2Cr cross reaction is shown in Figure 1.

A radio-frequency sweep was used to eject all nonreactant ions from the cell prior to collection of kinetic data, assuring that the rate of formation of the product ion was due only to the reactant parent ion.

Treatment of Data. The use of ratios, R_t, in the treatment of data yielding second-order rate constants has two distinct advantages. Most complications arising from nonreactive ion loss are alleviated, and the effect of instrumental fluctuation is minimized.

The derivation of the equations used to calculate rate constants is given in the Appendix. The rate of loss of a given ion is related to the masses of the ion and neutrals present in the cell.[46] Generally, the larger the mass of the ion, the more slowly it is lost from the cell. In the self-exchange process, rate constants for ion loss of the reactant (k_λ) and product (k_λ') isotopes are effectively the same since their masses do not differ by more than a few atomic mass units. The equation for rate constant determination (A5) then reduces to that of eq 1. In this case, the ratio treatment is an experimental advantage because kinetic runs that would normally be needed to determine k_λ are not necessary.

Care must be taken in examining the effect of the ratio treatment on the determination of cross reaction rate constants. The most important point is the comparison of Δk_λ ($=k_\lambda - k_\lambda'$) and k_1 (eq A5). If Δk_λ is small in relation to k_1, then determination of the rate constant will be valid without actually determining k_λ or k_λ'. Under the reaction conditions discussed above, no significant loss of ions takes place over the time scale of the reaction. The value of k_λ for the loss of any metallocene is therefore small in comparison to k_1; furthermore, the difference, Δk_λ, for any two metallocenes is very small, and no significant error is introduced into the calculated rate constants.

The use of the ratio R_t also reduces the error resulting from fluctuations in the number of ions produced in each step of the data acquisition. The nature of the FTICR detection technique necessitates starting the reaction at $t = 0$ and detecting ion populations at the time of interest. After each detection, all ions are removed from the cell and the sequence is repeated with a longer reaction time. If the loss or gain of any one ion is followed, fluctuations in the number of ions initially produced by the electron beam would appear as an increase in uncertainty in the rate constant. In contrast, the ratio of the reactant ion to the product ion is independent of the total number of ions, and less scatter is observed in the kinetic plots.

We have also considered carefully the effects of mass-dependent efficiencies in ion detection. A large difference in detection efficiencies between any two ions would produce a slight, characteristic curvature in the kinetic plot. However, we have found no evidence in our data that would indicate any significant error due to this effect. At the end of a given reaction under our conditions, the total integrated ion count was usually close to that measured in the initial detection used for $t = 0$.

Rate Constants. The rate constants for self-exchange reactions are given in Table I. Absolute rate constants are estimated to have errors of ±30%.

The measurement of the $Cr(CO)_6^{+/0}$ self-exchange rate was hampered by extensive fragmentation (CO loss) at all but the lowest electron impact energies. Large yields of the parent ion were therefore produced by charge-transfer ionization using $C_6H_6^+$ (C_6H_6 adiabatic IP = 9.2 eV)[47] to obtain higher signal-to-noise data. The pressure of benzene reagent gas ($\sim 10^{-6}$ torr) also

Table I. Gas-Phase Electron Self-Exchange Rates

reactants[a]	k_f, cm^3 molec^{-1} s^{-1}	k_f, M^{-1} s^{-1}	eff, k_f/k_L[b]
$Cp_2Cr^{+/0}$	4.8×10^{-10}	2.9×10^{11}	0.48
$Cp_2Mn^{+/0}$	1.3×10^{-12}[c]	8.0×10^{9}	0.013
$Cp_2Fe^{+/0}$	2.7×10^{-10}[c]	1.5×10^{11}	0.27
$Cp_2Co^{+/0}$	7.8×10^{-10}[c]	4.6×10^{11}	0.78
$Cp_2Ni^{+/0}$	6.5×10^{-10}	4.0×10^{11}	0.65
$Cp_2Ru^{+/0}$	2.5×10^{-10}[c]	1.5×10^{10}	0.25
$(Me_5Cp)_2Mn^{+/0}$	3.1×10^{-10}	1.8×10^{11}	0.28[d]
$(MeCp)_2Mn^{+/0}$	4.2×10^{-11}	2.5×10^{10}	0.04[e]
$Cr(CO)_6^{+/0}$	2×10^{-10}	6×10^{10}	0.15[f]
$SF_6^{-/0}$	$<5 \times 10^{-14}$[g]	$<3 \times 10^{7}$	$\lesssim 5 \times 10^{-5}$

[a] Abbreviations: Cp = cyclopentadienyl; Me_5Cp = pentamethylcyclopentadienyl; MeCp = methylcyclopentadienyl. [b] Assuming $k_L = 1.0 \times 10^{-9}$ cm^3 s^{-1} for the bis(cyclopentadienyl) metallocenes. [c] Value different from that reported in ref 32 due to subsequent improvements in system pressure calibration. [d] Polarizability of neutral unknown. From theoretical estimates (ref 49), k_L is estimated as 1.1×10^{-9} cm^3 s^{-1}. [e] Assuming $k_L = 1 \times 10^{-9}$ cm^3 s^{-1}. [f] Assuming $k_L = 1.3 \times 10^{-9}$ cm^3 s^{-1} (ref 49). [g] Not measurable with a SF_6 pressure of 10^{-6} torr and long reaction times.

(46) Sharp, T. E.; Eyler, J. R.; Li, E. *Int. J. Mass Spectrom. Ion Phys.* **1972**, *9*, 421.

(47) Levin, R.; Lias, S. G. *Ionization Potential and Appearance Potential Measurements 1971–1981*; National Bureau of Standards: Washington, D.C., 1982.

Table II. Rates of Gas-Phase Cross Reactions $L_2M + L_2M'^+ \rightarrow L_2M^+ + L_2M'$

L_2M[a]	L_2M'[a]	$\Delta E°$, eV[b]	k_f, cm^3 molec^{-1} s^{-1}	eff, k_f/k_L[c]
Cp_2Co	Cp_2Ru	−1.9	1.5×10^{-9}	1.5
Cp_2Cr	Cp_2Ru	−1.8	7.7×10^{-10}	0.6
Cp_2Cr	Cp_2Fe	−1.2	1.2×10^{-9}	1.2
Cp_2Ni	Cp_2Ru	−1.0	4.5×10^{-10}	0.5
Cp_2Cr	Cp_2Ni	−0.8	1.4×10^{-9}	1.4
Cp_2Fe	Cp_2Ru	−0.6	4.7×10^{-10}	0.5
Cp_2Mn	Cp_2Fe	−0.6	5.0×10^{-10}	0.5
Cp_2Mn	Cp_2Ni	−0.05[d]	3.1×10^{-11}	0.031
Cp_2Ni	Cp_2Mn	0.05[d]	1.3×10^{-11}	0.013
$(Me_5Cp)_2Mn$	Cp_2Ru	−2.1	5.5×10^{-10}	0.42[e]
$(Me_5Cp)_2Co$	Cp_2Ru	−2.8	8×10^{-10}	0.6[e]

[a] Abbreviations as in Table I. [b] Estimated as Δ(vertical IP). [c] Using $k_L = 1.0 \times 10^{-9}$ cm^3 s^{-1}. [d] Experimentally determined value of $\Delta G°$ at 375 K. [e] Assuming $k_L = 1.3 \times 10^{-9}$ cm^3 s^{-1} (see ref 49).

provided for rapid thermalization of the $Cr(CO)_6^+$ ion population. Ionization using smaller and more exoergic charge-transfer ions (e.g., NO^+ (IP = 9.26 eV) or CS_2^+ (IP = 11.2 eV))[47] resulted in increased fragmentation. The $SF_6^{-/0}$ self-exchange reaction is so slow that the rate constant cannot be measured on the time scale available by using the present ICR technique.

Table II gives rate constants measured for cross reactions. The $\Delta E°$ values for these reactions are estimated from the vertical ionization potentials. In general, the vertical IP values are not indicative of the actual driving force, but the more applicable *adiabatic* IP values are not available. Values for the $\Delta E°$ for the manganocene/nickelocene cross reaction are determined from direct equilibrium measurements and therefore are $\Delta G°$ values. Available spectroscopic data are inadequate for confident estimation of $\Delta S°$, and thus $\Delta H°$, for this latter equilibrium.

Also included in Tables I and II are the efficiencies of the reactions, defined as the ratio of the measured rate constant to an estimated collision rate. Estimates for the Langevin collision rate constant, $k_L = 2\pi(e^2\alpha/\mu)^{1/2}$, where e is the electron charge, α is the neutral polarizability, and μ is the reduced mass,[48] were based on theoretical polarizabilities for the decamethylmetallocenes and $Cr(CO)_6$.[49] For the other metallocenes, some of the cross reaction rate constants in Table II appear to exceed the estimated k_L values. It would be tempting to conclude that these results imply electron transfer taking place at distances beyond the critical impact parameter for neutral capture by the ion. However, given the probable errors in the calculated values of k_L for these complex ion/molecule collisons and the estimated errors in the measured rate constants, we do not believe these fast reactions occur at rates significantly in excess of the capture rate.

Discussion

Theory of Gas-Phase Electron Transfer. A simple theoretical model for gas-phase electron transfer has been presented previously,[33] and only a brief recapitulation will be given here.

A variety of considerations suggests that gas-phase electron transfer at thermal energies proceeds via a long-lived precursor complex for which the rate of formation can be estimated via Langevin,[48] average dipole orientation,[48a] or related schemes.[50] In support of this description, it is noted that the vast majority of thermal gas-phase electron-transfer reactions studied to date do not proceed with rate constants exceeding the estimated collision rates.[23] Therefore, electron transfer at distances beyond the critical impact parameter for ion capture ($b_c = 4e^2\alpha/\mu v_0^2$, where v_0 is the relative velocity)[48] by a neutral does not contribute significantly to the overall rates.[23] More rigorous evidence for a long-lived precursor complex has been presented by McMillan and Coplan[51] for the He^+/CO_2 dissociative charge-transfer reaction. In their studies, He^+ with a kinetic energy of 8.7 eV gave product ions (O^+ and CO^+) which had symmetrical fluxes with respect to the center of mass of the He^+/CO_2 system. Given that thermal electron transfer occurs with much lower average relative ion/molecule velocities (~0.03 eV), the formation of a precursor complex appears to be highly likely. In addition, many other types of ion/molecule reactions are best understood in terms of such a long-lived complex.[52-54]

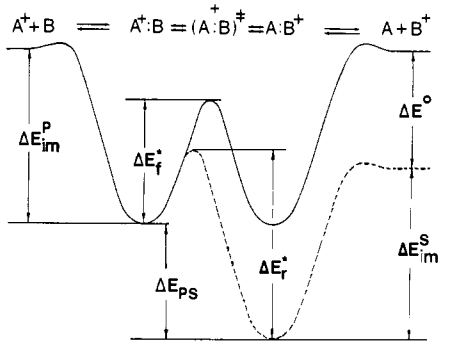

Figure 2. Potential surface for gas-phase electron-transfer reactions.[33] The solid line is appropriate for a symmetrical reaction (A = B) while the dashed line corresponds to an exothermic reaction with an exoergicity $\Delta E°$. The quantities $\Delta E_{im}{}^P$ and $\Delta E_{im}{}^S$ are the stabilities of the precursor complex (P) and the successor complex (S), respectively. The energy difference between precursor and successor minima is given by ΔE_{PS}. The height of the intrinsic potential barrier to electron transfer between the P and S states in the forward direction is given by the value of ΔE^*_f. For the reverse reaction in the exothermic case, the barrier is indicated as ΔE^*_r. Centrifugal barriers in the effective potential for association of the P or S complexes are shown.

We have therefore proposed[33] the following mechanism for the reactions considered here (Scheme I).

Scheme I

$$A^+ + B \underset{k_d}{\overset{k_L}{\rightleftharpoons}} A^+ - B \underset{k_{et}'}{\overset{k_{et}}{\rightleftharpoons}} A - B^+ \underset{k_L'}{\overset{k_d'}{\rightleftharpoons}} A + B^+$$

The rate constant k_L is the Langevin capture rate constant,[48] k_d and k_d' are dissociation rate constants for the precursor and successor complexes, respectively, and k_{et} and k_{et}' are the rate constants for electron exchange between the donor and acceptor centers in the collision complex. Assuming the steady-state approximation for the precursor and successor complexes, the overall forward bimolecular rate constant, k_f, is given for Scheme I by eq 9. When the reaction is exoergic and the condition $k_{et}'/k_d \ll$

$$k_f = \left(\frac{k_{et}k_d'}{(k_d + k_{et})k_d' + k_{et}'k_d} \right) k_L \qquad (9)$$

$(k_d + k_{et})k_d'$ holds, two limiting cases are found. If $k_{et} \gg k_d$, then $k_f \simeq k_L$; if $k_d \gg k_{et}$, then eq 10 applies for the overall efficiency. For symmetrical reactions (A = B), the same limiting conditions yield $k_f = k_L/2$ and eq 10, respectively.

(48) (a) Su, T.; Bowers, M. T., In *Gas Phase Ion Chemistry*; Bowers, M. T., Ed.; Academic: New York, 1979; p 84. (b) Gioumousis, G.; Stevenson, D. P. *J. Chem. Phys.* **1958**, *29*, 294.

(49) Experimental values for the polarizabilities of decamethylmetallocenes and $Cr(CO)_6$ could not be found in the literature. However, theoretical polarizability calculations by the INDO method yield estimates of α for $(Me_5Cp)_2Fe$ and $Cr(CO)_6$ (Parkinson, W.; Zerner, M., private communication. See also: Nagarajan, G. *Bull. Soc. Chem. Belg.* **1981**, *90*, 1077) that can be used to calculate Langevin collision rates of 1.1 and 1.3×10^{-9} cm^3 s^{-1}, respectively.

(50) Su, T.; Chesnavich, W. J. *J. Chem. Phys.* **1982**, *76*, 5183.

(51) McMillan, M. R.; Coplan, M. A. *J. Chem. Phys.* **1979**, *71*, 3063.

(52) E.g., nucleophilic displacements: (a) Dodd, J. A.; Brauman, J. I. *J. Phys. Chem.* **1986**, *90*, 3559. (b) Dodd, J. A.; Brauman, J. I. *J. Am. Chem. Soc.* **1984**, *106*, 5356. (c) Pellerite, M. J.; Brauman, J. I. *J. Am. Chem. Soc.* **1983**, *105*, 2672. (d) Pellerite, M. J.; Brauman, J. I. *J. Am. Chem. Soc.* **1980**, *102*, 5993. (e) Olmstead, W. N.; Brauman, J. I. *J. Am. Chem. Soc.* **1977**, *99*, 4219. (f) Caldwell, G.; Magnera, T. F.; Kebarle, P. *J. Am. Chem. Soc.* **1984**, *106*, 959.

(53) E.g., proton transfer: (a) Jasinski, J. M.; Brauman, J. I. *J. Am. Chem. Soc.* **1980**, *102*, 2906. (b) Kebarle, P. *Annu. Rev. Phys. Chem.* **1977**, *28*, 445. (c) Farneth, W. E.; Brauman, J. I. *J. Am. Chem. Soc.* **1976**, *98*, 7891.

(54) E.g., formation of ion/molecule complexes: (a) Jasinski, J.; Rosenfeld, R. N.; Golden, D. M.; Brauman, J. I. *J. Am. Chem. Soc.* **1979**, *101*, 2259. (b) Olmstead, W. N.; Lev-On, M.; Golden, D. M.; Brauman, J. I. *J. Am. Chem. Soc.* **1977**, *99*, 992.

$$\text{eff} = \frac{k_f}{k_L} = \frac{k_{et}}{k_d + k_{et}} \quad (10)$$

The distance dependence of gas-phase electron transfer has been considered in various theoretical models. With respect to Scheme I, the critical impact parameter b_c for the thermal ion/molecule reaction $Cp_2Fe^+ + Cp_2Fe$ can be estimated as ~12 Å, and the value of the maximum encounter distance for a capture of Cp_2Fe^+ by Cp_2Fe ($r_c = b_c/\sqrt{2}$) is ~8 Å. Any average velocity collision with b values less than ~12 Å will result in an impact (spiralling collision) between the ion and neutral.[48] The absence of electron-transfer rate constants in significant excess of the Langevin collision rate constant in our results (Tables I and II) suggests that ion/neutral encounters with encounter distances in excess of ~8 Å do not contribute significantly to the process. The "reactive" precursors are therefore assumed to result from intimate collisions between ions and neutrals. In contrast to electron-exchange reactions of small atomic reactants (e.g., $He + He^+$ [13,27b]), those of large polyatomic species feature relatively weak electronic interactions and the dominance of perturbative interactions by ion-induced dipole forces.

A potential surface for Scheme I is shown in Figure 2.[33] This general type of double well surface has been used extensively and successfully to rationalize rates of displacement reactions[52] and proton transfer[53] in ion/molecule processes. In our nomenclature, ΔE_{im}^P and ΔE_{im}^S are the stabilities of the precursor and successor complexes, $\Delta E°$ is the overall energy difference for infinitely separated reactants and products, and ΔE^*_f and ΔE^*_r are the classical intrinsic barriers to electron exchange in the forward and reverse directions, respectively. The value of ΔE_{PS} is the potential energy difference between the reactant (precursor) and product (successor) complexes. In the general asymmetrical case, $\Delta E°$ is not necessarily equal to ΔE_{PS}; therefore, it is not required that the energetics of the reactants and products in the electron-transfer process be given by the overall exoergicity. Such a situation would be especially likely when the reactant and product neutrals have much different polarizabilities (as in atomic ion/polyatomic neutral reactions, for example). Finally, the effective potential for the dissociation of precursor or successor complexes includes a centrifugal barrier when the appropriate rotational quantum number J is non-zero.[55-57]

The overall efficiency of the bimoleular reaction in Scheme I depends on the relative values of the electron-transfer rate constant, k_{et}, and the dissociation rate constant for the precursor complex $[A^+ - B]$, k_d (eq 10). If the value of ΔE^*_f is large compared to $|\Delta E_{im}^P|$, the forward reaction will have a positive activation barrier and the reaction will usually be inefficient. In addition, inefficient reactions may occur when $|\Delta E_{im}^P| - \Delta E^*_f$ is positive for reasons discussed elsewhere.[52,53,58] For exoergic reactions, ΔE_{PS} may be negative, and the value of ΔE^*_f will be reduced for increasing values of $-\Delta E_{PS}$ in the normal exoergic region ($|\Delta E°| \leq 4\Delta E^*_0$, where ΔE^*_0 is the intrinsic central barrier if $\Delta E° = 0$). For a cross reaction with a negligible entropy change, $\Delta S°$, eq 11 holds, where $\gamma = \Delta E_{PS}/(4\Delta E^*_1 + 4\Delta E^*_2)$.[59] ΔE^*_1 and ΔE^*_2 are the intrinsic central barriers for the corresponding self-exchange reactions for the two reactants.

$$\Delta E^*_f = \frac{\Delta E^*_1 + \Delta E^*_2}{2} + \frac{\Delta E_{PS}}{2}(1 + \gamma) = \Delta E^*_0 + \frac{\Delta E_{PS}}{2}(1 + \gamma) \quad (11)$$

Self-Exchange Reactions. In the development of theoretical models for electron-transfer reactions, self-exchange reactions have provided critical tests for theories and a basis for futher consideration of cross reactions.[1-5] Thus, we have determined the rates of a number of gas-phase self-exchange reactions to provide a point of departure for later studies of various electron-transfer phenomena.

The $SF_6^{-/0}$ exchange reaction rate constant could not be determined with our technique (eff $< 5 \times 10^{-5}$), which is intrinsically limited by ion loss from the ion trap. A somewhat higher upper limit was put on this self-exchange reaction by other workers (eff $\lesssim 10^{-3}$).[60] The large kinetic barrier implied by this result is most likely related to the significant bond length changes which occur upon reduction of SF_6 to SF_6^-.[61] A theoretical intrinsic reorganization barrier ΔE^* (~1.0 eV) can be estimated by using a combination of experimental and theoretical bond lengths and frequencies.[33] The ground-state geometry of SF_6^- is still an open question,[61] so further refinement of the model for the activated complex is not profitable at this time. Assuming the electronic interaction in the precursor complex is sufficient for an adiabatic reaction,[1,2] we believe the expected large intrinsic Franck–Condon barriers are the principal cause of the low self-exchange rate at thermal energies.

For the metallocenes, the self-exchange efficiencies are all high (>0.2) with the exception of $Cp_2Mn^{+/0}$ and $(MeCp)_2Mn^{+/0}$. The estimation of k_L is difficult for most organometallics since very little experimental data for polarizabilities are available. For the bis(cyclopentadienyl) compounds, the average polarizability, α, of ferrocene[62] was used in all cases, since the d^n configuration will likely have only a small effect on α. Most of the measured values of k_f are within experimental error of the maximum rate $k_L/2$ and are close to half of many of the measured rates of related cross reactions (vide infra). Therefore, we assume that many of the self-exchange reactions are near the collisional limit of efficiency. The rate constants for $Cp_2Fe^{+/0}$ and $Cp_2Ru^{+/0}$ have been investigated repeatedly and are always found to be somewhat lower than those of the other $Cp_2M^{+/0}$ reactions with M = Cr, Co, and Ni. The origin of this difference is not clear, although it may be associated with variations in $\Delta E^* - |\Delta E_{im}|$ (Figure 2). The differences are small in any case, being just outside the estimated error limits (±30%). From available and estimated structural and vibrational data, most metallocenes are predicted to have ΔE^* values $\lesssim 1.0$ kcal mol^{-1}.[63] Given the significant polarizabilities of these molecules, this barrier is likely much less than $|\Delta E_{im}^P|$ (Figure 2). In the terminology of unimolecular rate theory,[55-57] the activated complex is not especially "tight" in comparison to the loose-orbiting dissociative transition state. The rate constant k_{et} in Scheme I is therefore large in comparison to k_d, and the observed rates are at or near the maximum, $k_L/2$.

The efficiencies for the self-exchanges $Cp_2Mn^{+/0}$ and $(MeCp)_2Mn^{+/0}$ are significantly below collisional. The manganocenes are unusual among the metallocenes as they have low-lying high-spin states ($^6A_{1g}$)[64-68] (this discussion will assume D_{5d} sym-

(55) Beynon, J. H.; Gilbert, J. R. *Application of Transition State Theory to Unimolecular Reactions*; Wiley: Chichester, 1984.
(56) Robinson, P. J.; Holbrook,, K. A. *Unimolecular Reactions*; Wiley-Interscience: New York, 1972.
(57) Forst, W. *Theory of Unimolecular Reactions*; Academic: New York, 1973.
(58) Mautner, M. In *Gas Phase Ion Chemistry*; Bowers, M. T., Ed.; Academic: New York, 1979; p 197.
(59) Marcus, R. A.; Sutin, N. *Inorg. Chem.* **1975**, *14*, 213.
(60) (a) Foster, M. S.; Beauchamp, J. L. *Chem. Phys. Lett.* **1975**, *31*, 482. (b) Lifshitz, C.; Tiernan, T. O.; Hughes, B. M. *J. Chem. Phys.* **1973**, *59*, 3182–3192.
(61) (a) Hay, P. J. *J. Chem. Phys.* **1982**, *76*, 502. (b) Drzaic, P. S.; Brauman, J. I. *Chem. Phys. Lett.* **1981**, *83*, 508–511. (c) Drzaic, P. S.; Brauman, J. I. *J. Am. Chem. Soc.* **1982**, *104*, 13–19.
(62) LeFevre, R. J. W.; Murthy, D. S. N.; Saxby, J. D. *Aust. J. Chem.* **1971**, *24*, 1057.
(63) Calculated by using eq 5 or 6 in ref 33. Note that these equations apply only for symmetrical reactions (A = B in Scheme I) for which $\Delta E_{PS} = 0$ ("ΔE_{RP}" in ref 33). In ref 33, the text and Figure 2 caption imply that the classical inner reorganizational barrier ($4\Delta E_{in}^* = {}^1/_2\Sigma_i f_i \Delta r_i^2$) can be used to estimate ΔE_f^* for cases where $\Delta E_{PS} \neq 0$. This relation actually calculates only an intrinsic reorganizational barrier (ΔE^*_0 in this Discussion) which must be corrected for non-zero values of ΔE_{PS} (eq 11 in this Discussion or eq 11 and 12 of ref 33).
(64) Haaland, A. *Acc. Chem. Res.* **1979**, *12*, 415.
(65) Hebendanz, N.; Köhler, F. H.; Müller, G.; Riede, J. *J. Am. Chem. Soc.* **1986**, *108*, 3281.
(66) Ammeter, J. H.; Buchen, R.; Oswald, N. *J. Am. Chem. Soc.* **1974**, *96*, 7833.
(67) Switzer, M. E.; Wang, R.; Rettig, M. F.; Maki, A. H. *J. Am. Chem. Soc.* **1974**, *96*, 7669.

metries apply). Studies of the permethylated species $(Me_5Cp)_2Mn$ show that it is essentially low-spin $^2E_{2g}$,[69] and the predicted M–L distance changes lead to a relatively low value of ΔE^*_f (0.3 kcal mol^{-1}).[33] Jahn–Teller distortions have been noted for this species[70] but have not been taken into account in the estimate of ΔE^*_f. The observed efficiency for the $(Me_5Cp)_2Mn^{+/0}$ exchange is high, as expected (Table I).

Manganocene and dimethylmanganocene have significant amounts of high-spin and low-spin states in equilibrium near room temperature. The UV photoelectron spectrum of Cp_2Mn vapor at 60 °C suggests a value of K_{eq} for eq 12 of ~0.005.[71] Only

$$Cp_2Mn(^6A_{1g}) \rightleftarrows Cp_2Mn(^2E_{2g}); \quad K_{eq} = \frac{[^2E_{2g}]}{[^6A_{1g}]} \qquad (12)$$

the $^6A_{1g}$ state can be detected by EPR down to 4.2 K when Cp_2Mn is doped into Cp_2Mg.[67] For $(MeCp)_2Mn$ in the gas phase, the value of K_{eq} has been estimated from electron diffraction results to be ~0.61 at 100 °C,[72] and K_{eq} decreases with increasing temperature.[73] The $^6A_{1g} \rightleftarrows {}^2E_{2g}$ equilibrium for $(MeCp)_2Mn$ has been studied in solution[65-67] by EPR and NMR. Hebendanz et al.[65] used the latter method to obtain the thermodynamic parameters $\Delta H° = -2.8$ kcal mol^{-1} and $\Delta S° = -10.7$ cal deg^{-1} mol^{-1}. These parameters yield a K_{eq} of 0.20 at 100 °C, which is much smaller than the gas-phase result. Thermodynamic parameters were obtained by Switzer et al.[67] for $(MeCp)_2Mn$ in toluene by using EPR ($\Delta H° = -1.8 \pm 0.1$ kcal mol^{-1}, $\Delta S° = -5.8 \pm 0.6$ cal deg^{-1} mol^{-1}, and K_{eq} (100 °C) = 0.61). The high-spin form is favored entropically (apparently due to orbital and spin degeneracies, $R \ln {}^6/_4 = 0.8$ cal deg^{-1} mol^{-1} and lower M–L vibrational frequencies in the high-spin form[64]), but the ground state of $(MeCp)_2Mn$ is low-spin.

The spin-interconversion equilibrium $^6A_{1g} \rightleftarrows {}^2E_{2g}$ for the manganocenes is established prior to the ion/molecule collisions and may be the controlling factor in the electron-transfer process. On the basis of the observations made for other metallocenes, the self-exchange process of eq 13 should proceed with near-collisional

$$Cp_2MnCp_2Mn(^2E_{2g}) + {}^*Cp_2Mn^+(^3E_{2g}) \rightleftarrows Cp_2Mn^+(^3E_{2g}) + {}^*Cp_2Mn(^2E_{2g}) \qquad (13)$$

efficiency since the M–Cp distortion for the $^2E_{2g}/{}^3E_{2g}$ transition will be small. On the other hand, the high-spin/low-spin exchange has a large M–Cp distortion (~0.25 Å) and should have a ΔE_f^* of ~9 kcal mol^{-1},[33] which will likely reduce k_f significantly. In addition, reaction 14 has spin multiplicity restrictions that may

$$Cp_2Mn(^6A_{1g}) + {}^*Cp_2Mn^+(^3E_{2g}) \rightleftarrows Cp_2Mn^+(^3E_{2g}) + {}^*Cp_2Mn(^6A_{1g}) \qquad (14)$$

make the process strongly nonadiabatic and reduce k_{et}. In both $Cp_2Mn^{+/0}$ and $(MeCp)_2Mn^{+/0}$, a possible pathway for electron exchange is then via the spin preequilibrium (12) followed by the low-spin/low-spin exchange (eq 13). Assuming a value of k_f for eq 13 of ~3 × 10^{-10} cm^3 s^{-1}, expected values of k_{obsd} for this mechanism are 1.5 × 10^{-12} cm^3 s^{-1} for $Cp_2Mn^{+/0}$ (observed 1.3 × 10^{-11} cm^3 s^{-1}) and 2 × 10^{-10} cm^3 s^{-1} for $(MeCp)_2Mn$ (observed 4.2 × 10^{-11} cm^3 s^{-1}). Given the estimates and approximations involved, it is reasonable to conclude the neutral low-spin forms can contribute significantly to the observed overall exchange rate.

Cross Reactions in the Normal Region. Investigations of cross reactions have often focused on the effect of exoergicity on the rates of electron-transfer reactions in solution.[1,2] For most metal complexes studied, the Marcus cross relation ($k_{12} \simeq (k_{11}k_{22}K_{12})^{1/2}$ for low exoergicities) has proved consistent in its prediction of the dependences of cross-reaction rate constants (k_{12}) on the equilibrium constants (K_{12}) and self-exchange rate constants (k_{11}, k_{22}) for the individual reactants.[74,75] Occasional exceptions have been noted for the reactions of some smaller redox couples (e.g., $O_2^{0/-}$).[76]

Given the complexity of predicting rate constants for gas-phase electron transfer from estimated potential surfaces, a simple analogue of the cross relation is not as yet available for the gas-phase system.[77] However, it is reasonable to consider the effect of exoergicity on the central barriers, ΔE^*_f and ΔE^*_r. Thus, the energy difference ΔE_{PS} (Figure 2) becomes crucial. In discussing cross reactions of the metallocenes, we will assume that $\Delta E_{PS} \simeq \Delta E°$ since the values of $\Delta E_{im}{}^P$ and $\Delta E_{im}{}^S$ are expected to be similar in the series.

Increasing exoergicity in cross reactions will lower the height of the central barrier (Figure 2 and eq 11), thereby increasing the rate k_{et} in Scheme I in the normal region of relatively low driving force.[1] For reactions where the condition $k_{et} < k_d$ is met, eq 10 applies, and the overall efficiency will increase at higher driving forces.[33] The data reported by Grimsrud et al.[34] clearly reflect this trend for the gas-phase cross reactions between SF_6^- and various organic acceptors.

Our data for cross reactions involving $Cp_2Mn^{+/0}$ also show the expected dependence on $\Delta E°$ (Table II). In these reactions, the probable role of a spin equilibrium in Cp_2Mn must be considered. For example, in the Cp_2Mn/Cp_2Ni^+ reaction, the low exoergicity will not lower the central barrier substantially from the value $(\Delta E^*_{Mn} + \Delta E^*_{Ni})/2$ (eq 11). The spin equilibrium path likely contributes in that case if the ΔE^*_f value for the cross reaction (~4 kcal mol^{-1}) still retards the direct exchange for high-spin Cp_2Mn. The efficiency of the cross reaction (0.031) is comparable to the statistically corrected efficiency of the $Cp_2Mn^{+/0}$ self exchange (0.026) and suggests a similar mechanism. For the endoergic reaction Cp_2Ni/Cp_2Mn^+, the efficiency (0.013) is less than that of the $Cp_2Mn^{+/0}$ self exchange, possibly reflecting the balance between the unfavorable thermodynamics and the lower intrinsic central barrier in the cross reaction.

For the cross reaction Cp_2Mn/Cp_2Fe, the exoergicity is expected to eliminate the central barrier for the $^6A_{1g}(Cp_2Mn)/{}^2E_{2g}(Cp_2Fe^+)$ reactions (i.e., $-\Delta E° \gtrsim 4\Delta E^*_0$). Therefore, the spin equilibrium probably is not as important and the observed efficiency (Table II) is high, reflecting the participation of the high-spin state in the precursor-to-successor transition.

Cross Reactions in the Inverted Region. One of our goals in studying gas-phase electron transfer is to provide insights into aspects of condensed-phase redox reactions which may be obscured by the presence of a solvent. It appears that these studies can be useful in investigating bimolecular electron-transfer reactions in the highly exoergic region where classical, semi-classical, and quantum theories predict a falloff of rates with increasing driving force.[1,3,39] In particular, the roles of excited states and Franck–Condon factors are rather easily described for gas-phase reactants since techniques such as photoelectron spectroscopy[78-80] (for

(68) The possibility that ring exchange provides a pathway for isotope exchange for the high-spin states requires that the given rate constants are strictly upper limits for the electron-exchange rate constants.[64] However, ring exchange apparently does not provide a pathway for the other low-spin metallocenes which have multiple metal isotopes, and ring exchange involving the low-spin manganocenium reactants is unlikely. Manganocene undergoes a facile ring exchange in the gas phase (Sharpe, P.; Richardson, D. E., unpublished results). When introduced simultaneously into the mass spectrometer, manganocene and perdeuteriated manganocene give a positive ion spectrum which is consistent with statistical redistribution of the Cp rings prior to electron impact. Since manganese is isotopically pure (100% ^{55}Mn), no natural abundance metal isotopes can be used to follow the self-exchange process. Therefore, the m + 1 isotope (^{13}C–Cp) was used to follow the reactions. The low-spin ionic form, Cp_2Mn^+, should be less prone to Cp exchange than the high-spin, neutral Cp_2Mn. For example, no evidence for ring exchange in $(Me_5Cp)_2Mn^{+/0}$ reactions is found.

(69) Smart, J. C.; Robbins, J. L. *J. Am. Chem. Soc.* **1978**, *100*, 3936.

(70) Freyberg, D. P.; Robbins, J. L.; Raymond, K. N.; Smart, J. C. *J. Am. Chem. Soc.* **1979**, *101*, 892.

(71) Evans, S.; Green, M. L. H.; Jewitt, B.; King, G. H.; Orchard, A. F. *J. Chem. Soc., Faraday Trans. 2* **1974**, *70*, 356.

(72) Almemingen, A.; Haaland, A.; Samdal, S. *J. Organomet. Chem.* **1978**, *149*, 219.

(73) Cauletti, C.; Green, J. C.; Kelly, M. R.; Powell, P.; van Tilborg, J.; Robbins, J.; Smart, J. *J. Electron Spectrosc. Relat. Phenom.* **1980**, *19*, 327.

(74) Chou, M.; Creutz, C.; Sutin, N. *J. Am. Chem. Soc.* **1977**, *99*, 5615.

(75) Weaver, M. J.; Yee, E. L. *Inorg. Chem.* **1980**, *19*, 1936.

(76) (a) McDowell, M. S.; Espenson, J. H.; Bakac, A. *Inorg. Chem.* **1984**, *23*, 2232. (b) Ram, M. S.; Stanbury, D. M. *J. Phys. Chem.* **1986**, *90*, 3691.

(77) Dodd and Brauman (ref 52a) have developed a modification of eq 11 which correlates driving force and overall rates in certain limited cases of nucleophilic displacement reactions.

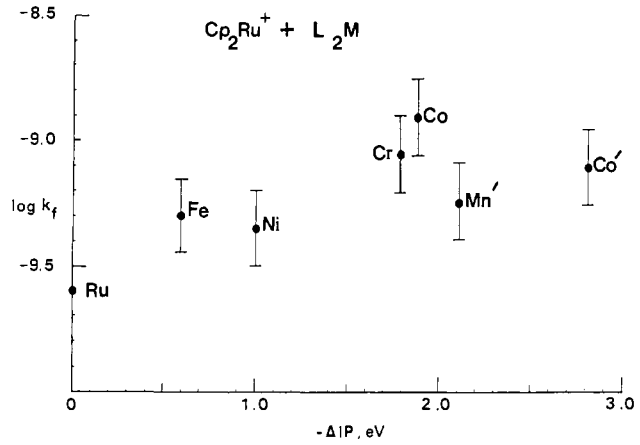

Figure 3. Plot of log k_f vs. $\Delta E°$ for cross reactions (L_2M/Cp_2Ru^+) where L = Cp or Me_5Cp. The $\Delta E°$ values are approximated by the difference in vertical ionization potentials for the metallocenes. The identity of M is indicated for each point, Mn′ and Co′ are $(Me_5Cp)_2M$ compounds, and the rest are Cp_2M. Estimated error bars are shown for the rate constants.

cationic reactants) or photodetachment in negative ion beams[81] (for anionic reactants) can in principle provide direct information about these relevant properties for neutral/ion conversions.

A strong dependence of reaction rates on $\Delta E°$ in electron-transfer reactions has been observed in the gas phase for small molecules and atoms in both thermal and ion-beam experiments.[12,19,21,23,30,31] For example, the cross sections for electron transfer from NH_3 to various accelerated ions with recombination energies (RE, the energy released in the process $A^+ + e^- \rightarrow A$) of ~10.5–16 eV cover a range of a factor of ~30.[30] The maximum rates are found with RE values at the maxima of NH_3 photoelectron peaks (e.g., Ar^+), and the minimum rates are found for RE values in the region between ionization manifolds (e.g., CO^+). From this and other reports,[19,21,23,30,31] it is clear that Franck–Condon factors for ionization processes are indeed important for bimolecular electron-transfer reactions of small molecules, and an "inverted" region definitely exists in those cases.

The rate constants were determined for a series of cross reactions with Cp_2Ru^+ as the acceptor (vertical IP = 7.45 eV,[73] adiabatic IP ≃ 7.0 eV[82]) and with approximate values of $\Delta E°$ in the range 0.5 to >2.5 eV (Figure 3 and Table II). For $Cp_2Ru^{+/0}$ and all of the donors chosen, the intrinsic barriers to their self-exchange reactions are expected to be small (≲1 kcal mol^{-1}), and the reactions are strongly in the inverted region energetically ($\Delta E°$ > 4 ΔE_0*). By use of eq 11, the predicted classical intersections for the imbedded zero-order surfaces which define the central barrier range from ~30 (Cp_2Fe/Cp_2Ru^+, $\Delta E°$ ≃ −0.6 eV) to ≳300 kcal mol^{-1} ($(Me_5Cp)_2Co/Cp_2Ru^+$, $\Delta E°$ ≃ −2.8 eV). Clearly, the classical barriers predicted by the simple two-surface model used to derive eq 11 do not influence these reactions, since the rate constants would be immeasurably slow for such large barriers. Quantum mechanical models based on the same two-surface description of the reactants and products have been derived,[1-3] and a roughly linear dependence of ΔE* on $\Delta E°$ is predicted in the inverted region (the energy gap law). However, a reduction in rates with very high driving forces is simply not seen in the cross reactions of Figure 3. The models do not seem capable of predicting the observed cross reaction rates for either the present systems or a large number of other bimolecular redox processes in solution.[40] In the following discussion, we suggest that the apparent failure of the models in the present case is primarily due to *an inadequate theoretical description of the electronic and vibrational states of the reactants.*

The limitations of bimolecular kinetics in detecting an inverted region must be considered first. In solution reactions, the diffusion rate limits the observation of fast electron-transfer steps;[40] in the gas phase, the maximum observed rate is the ion/molecule collision rate. Both types of reactions are typically limited in the detectability of the rate maxima which characterize the onset of the inverted region (at $\Delta E° \simeq 2(\Delta E^*_1 + \Delta E^*_2)$, eq 11). However, given the rather steep falloff of the expected rates in the inverted region, a rate downturn is usually expected at some point beyond the maximum.[40] For example, if the lifetime of the gas-phase precursor complex in Scheme I is ~10^{-6} s, then an inefficient reaction will be observed when $k_{et} \lesssim 10^6$ s^{-1} (eq 10). Experimental values for precursor lifetimes have not yet been obtained for the present reactants, and theoretical estimation of k_d via a RRKM scheme[54] is not possible without values for ΔE_{im}. The rough estimate of 10^{-6} s is based on values derived[54a] for $(C_6H_6)_2^+$ by considering the increased number of degrees of freedom in dimer ions such as $(Cp_2Fe)_2^+$.

To explain the apparent failure of the simple model described above to predict the rapid bimolecular electron transfers in the predicted inverted region, we begin by considering a quantum model for the initial (precursor) to final (successor) state conversion. Given the large number of vibrational and rotational levels in the reactants considered here, the density of states in the final state can be taken as large, and these transitions can be therefore considered to be near the statistical limit for radiationless processes.[83] The probability of a transition from the initial vibronic state Pν of the precursor complex to a set of final state vibronic levels {Sω} of the successor complex is then given by the approximation of the Fermi golden rule[84] in eq 15, where H_{PS} is the

$$W_{P_\nu} = \frac{4\pi^2 H_{PS}^2}{h} \sum_\omega \langle \chi_\nu^P | \chi_\omega^S \rangle^2 \delta(E_\nu^P - E_\omega^S) \qquad (15)$$

integral describing the electronic coupling between the initial state P and the final state S and the δ function ensures energy conservation. The Franck–Condon factor $\langle \chi_\nu^P | \chi_\omega^S \rangle^2$ is the overlap integral of the vibrational wave functions χ for the vibronic levels ν and ω. To find the total transition probability, the energy distribution in the initial state must be incorporated, and the total transition probability is

$$W = \sum_\nu F(E_\nu) W_{P_\nu} \qquad (16)$$

where $F(E_\nu)$ is the appropriate energy distribution function for the initial state. Since third-body collisions with the precursor complex are rare in ICR experiments, the complex is necessarily "hot" due to chemical activation by kinetic energy released upon formation of the complex (ΔE_{im}, Figure 2). Expressions for $F(E_\nu)$ have been given elsewhere,[56,57] and chemical activation has been incorporated into models for other ion/molecule reactions.[52-54]

We now express the vibrational wave functions χ_ν^P and χ_ω^S as products of the individual reactant's vibrational wave functions

$$\chi_\nu^P = \chi^P{}_{n,k}\chi^P{}_{+,l} = |n,k\rangle|+,l\rangle$$
$$\chi_\omega^S = \chi^S{}_{n,p}\chi^S{}_{+,q} = |n,p\rangle|+,q\rangle \qquad (17)$$

and obtain eq 18. The symbols n and + refer to the neutral and

$$k_{et} = \frac{4\pi^2 H_{PS}^2}{h} \sum_k \sum_l \sum_p \sum_q F(E_{n,k}^P + E_{+,l}^P) |\langle n,k|+,q\rangle|^2$$
$$|\langle +,l|n,p\rangle|^2 \delta(E_{n,k}^P + E_{+,l}^P - E_{n,p}^S - E_{+,q}^S + \Delta E_{PS}) \qquad (18)$$

ionized states, respectively, and the vibrational quantum numbers are k, l, p, and q. The Franck–Condon overlap integrals $\langle n,k|+,q\rangle$

(78) Rabalais, J. W. *Principles of Ultraviolet Photoelectron Spectroscopy*; Wiley-Interscience: New York, 1977.
(79) Green, J. C. *Struct. Bonding (Berlin)* **1973**, *43*, 37.
(80) Cowley, A. H. *Prog. Inorg. Chem.* **1979**, *26*, 45.
(81) Mead, R. D.; Stevens, A. E.; Lineberger, W. C. In *Gas Phase Ion Chemistry*; Bowers, M. T., Ed.; Academic: New York, 1984; Vol. 3, Chapter 22.
(82) Adiabatic ionization potentials (aIP) for organometallic compounds are virtually unknown. An estimate for aIP can be obtained by extrapolation of the PE band on the low energy side. However, this procedure is subject to large errors due to the vertical nature of PE transitions. Substantial distortions in the excited state can make detection of the 0–0 transition difficult, and the true ionic ground state may have a multiplicity different from that of the predominantly observed state.
(83) Englman, R.; Jortner, J. *Mol. Phys.* **1970**, *18*, 145.
(84) Freed, K. F.; Gelbart, W. M. *Chem. Phys. Lett.* **1971**, *10*, 187.

and $\langle +,l|n,p\rangle$ then describe the overlaps of initial and final vibrational wave functions located on a *single* reactant.

The discussion above and eq 15–18 closely follow the development of nonadiabatic electron-transfer theory for solvated reactants.[3] Equation 18 differs from those usually presented for the solution case in the absence of terms relating to the solvent trapping and the replacement of the Boltzman distribution by the chemical activation distribution F. The energy sharing between solvent and reactants suggested by calculations[3,4] obviously is not present in the gas phase, but energy sharing will occur between the vibrational mode which tends to trap the electron and other thermally or chemically activated modes in the reacting complex.[56,57] A detailed analysis necessary to calculate values of k_{et} will not be attempted here, but we will consider the effect of the Franck–Condon factors in eq 18 on the overall transition probability.

Franck–Condon factors such as those in eq 18 can be obtained experimentally by using photoionization methods[78,85,86] or they can be estimated theoretically from a knowledge of the changes in structure and vibrational frequencies that occur upon ionization.[87] In theoretical modeling of the highly exoergic reactions in condensed phases, the latter approach generally has been taken. The gas-phase reactions studied here provide an opportunity to apply experimental Franck–Condon factors, since extensive photoelectron (PE) data are available for the metallocenes.[79] The quantitative limitations of using Franck–Condon factors from PE spectra have been discussed,[88] but in general the method gives a qualitative picture of the Franck–Condon manifold. In some cases, detailed analyses of PE vibrational structure can be carried out to obtain structural and vibrational information about organometallic ionic states.[89]

We begin by showing that the single harmonic oscillator model typically used to derive inner reorganizational barriers for electron-transfer reactions does not fully account for the observed FC manifold for the reactants considered here, as a model clearly must given the central importance of FC factors to the magnitude of k_{et}. For example, consider the theoretical FC factors for $Cp_2Fe \rightarrow Cp_2Fe^+$ calculated by using structural and vibrational data. If the Cp ring is considered as a rigid unit (a dubious but typical approximation[90]), the Fe–Cp bond distance changes 0.04 Å in the neutral–ion conversion.[65] With a vibrational frequency for the Cp–M–Cp A_{1g} stretch of 305 cm^{-1},[91] the full width at half-maximum (FWHM) for the first ionization band ($^1A_{1g} \rightarrow {}^2E_{2g}$, vertical IP = 6.86 eV) is predicted to be $\lesssim$0.15 eV.[92] The observed FWHM in the PE spectrum is 0.3–0.4 eV.[73] In addition, the $^2A_{1g}$ ion state overlaps significantly with the $^2E_{2g}$ state, yielding a FC manifold centered around 7 eV with an overall FWHM of ~0.6 eV.[73] The $^2A_{1g}$ excited state has not been observed in the optical spectrum of Cp_2Fe^+.[91,93] The broadening of the $^2E_{2g}$ state is at least partially the result of spin–orbit coupling as deduced from magnetic resonance studies and optical spectroscopy of Cp_2Fe^+ salts.[91] Some excitation of higher frequency Cp ring modes may also be associated with the ionization process and would lead to the broadening of the manifold. In addition, the Fe–C bond lengths may change more upon ionization in the gas phase than predicted by using crystallographic distances for Cp_2Fe^+ salts.[65] Photoionization and PE bands in this energy region measured for Cp_2Fe in solution have similar widths.[94] If the observed FC widths in the PE spectra result from a larger change in M–C bond lengths upon ionization in the gas phase than suggested by structural data, the calculated inner reorganization barriers must reflect this difference (increasing ΔE^*). Whether this increase would appear in the rate constants k_f depends on the degree to which k_{et} would be decreased. However, the presence of nearby electronic excited states (as a result of spin–orbit coupling or Jahn–Teller effects, for example) can broaden the FC manifold without altering activation barriers in self-exchange reactions.

The result of a broad FC manifold in $Cp_2Fe^{+/0}$ is relatively large FC factors $\langle n,k|+,q\rangle$ connecting the neutral state to the ion state when the ionization covers a range ~6.5 to ~7.5 eV. Assuming that the A_{1g} frequencies of the ion and neutral are approximately equal, the FC factors for the ion-to-neutral conversion at the other center ($\langle +,l|n,p\rangle$) can be related to those of the ionization process.[95] Therefore, a substantially larger range of ΔE_{PS} values than suggested by the "theoretical" FC factors can be accommodated in cross reactions of $Cp_2Fe^{+/0}$ while still retaining significant FC overlaps and a relatively efficient electron-transfer probability. In contrast, the simple harmonic oscillator model discussed above would predict the onset of the inverted region to occur at *much lower values of* $-\Delta E_{PS}$.

For any reactants A and B, if the FC manifolds are broader than expected, a larger range of ΔE_{PS} values can still yield significant values for the vibrational overlap integrals in eq 18. Assuming $\Delta E_{PS} \simeq \Delta E°$ and small vibrational frequency differences between the neutral and ion states, *the PE spectra of reactants A and B can be used to identify A,B$^+$ combinations that have high FC factors and thus relatively efficient precursor to successor transitions*. In addition, the available energetically accessible electronic excited states of the ion can be identified. Formation of excited electronic states in products of solution electron-transfer reactions is well established[96] and has been suggested as an explanation for the absence of an inverted region in some reactions.[40]

Examination of the PE spectra[71,73] of the metallocenes studied here reveals that the relatively broad FC manifolds and the available electronically excited states can account for the efficient electron-transfer reactions in the nominal "inverted" region for the reactants in Figure 3. For example, the estimated $\Delta E°$ for the Cp_2Ru^+/Cp_2Ni reaction is −1.0 eV. If ~0.5 eV appears as vibrational excitation in the $^1A_{1g}$ electronic state of Cp_2Ru and $^2E_{1g}$ electronic state of Cp_2Ni^+ products, large FC factors would be expected based on the width of the PE bands. In the oxidation of Cp_2Cr by Cp_2Ru^+, the $\Delta E°$ of ~1.7 eV would be sufficient to produce electronically excited states of the ion Cp_2Cr^+ ($^2E_{2g}$ or $^2E_{1g}$ states of the d^3 configuration[73]). By use of the simple theoretical model and the predicted FC manifolds for these reactions, the calculated nuclear factors would be very small, and a low rate constant would be expected. Since values of $F(E)$ needed to predict k_{et} values in eq 18 cannot be calculated without a value for ΔE_{im}^P, the values of k_{et} cannot be estimated. However, as an example, the value of the nuclear factor[1] for the Cp_2Ru^+/Cp_2Ni reaction assuming $F(E)$ is the Boltzmann distribution is ~10^{-10}, using the semiclassical model.[1]

Beyond the limitations of bimolecular kinetics and the roles of excited states and FC manifolds, other factors must be considered in discussing the rates of gas-phase electron-transfer re-

(85) Eland, J. H. D.; Danby, C. J. *Int. J. Mass Spectrom. Ion Phys.* **1968**, *1*, 111.
(86) Coon, J. B.; DeWames, R. E.; Loyd, C. M. *J. Mol. Spectrosc.* **1962**, *8*, 285.
(87) For a detailed discussion of Franck–Condon factors in polyatomic molecules, see: Sharp, T. E.; Rosenstock, H. M. *J. Chem. Phys.* **1964**, *41*, 3453.
(88) Stockbauer, R.; Inghram, M. G. *J. Chem. Phys.* **1971**, *54*, 2242.
(89) Hubbard, J. L.; Lichtenberger, D. L. *J. Am. Chem. Soc.* **1982**, *104*, 2132.
(90) E.g., see: Li, T. T.; Weaver, M. J.; Brubaker, C. H. *J. Am. Chem. Soc.* **1982**, *104*, 2381.
(91) Duggan, D. M.; Hendrickson, D. N. *Inorg. Chem.* **1975**, *14*, 955.
(92) Relative intensities for the progression $^1A_{1g}$ (v_s = 0, 1, 2...) → $^2E_{2g}$ (v'_s = 0, 1, 2...) were calculated by using the harmonic oscillator model (ref 86). The relatively small distortion of the M–Cp distance in the ionized state would lead to the 0→0 and 0→1 transitions having most of the intensity near room temperature, and the overall bandwidths would be somewhat greater than $\sim 2h\nu \simeq 610$ cm^{-1}.
(93) The lowest energy state characterized for Cp_2Fe^+ by absorbance spectroscopy ($^2E_{1u} \leftarrow {}^2E_{2g}$) has its origin at ~1.9 eV (ref 91 and Sohn, Y. S.; Hendrickson, D. N.; Gray, H. B. *J. Am. Chem. Soc.* **1971**, *93*, 3603). The lowest doublet state observed in the ferrocene PE spectrum, $^2A_{1g}$, is at ~0.6 eV above the adiabatic ionization potential of the $^2E_{2g}$ state.
(94) Nemec, L.; Chia, L.; Delahay, P. *J. Phys. Chem.* **1975**, *79*, 2935.
(95) This is most easily seen in terms of displaced identical harmonic surfaces with different minima positions in the relevant normal coordinate space for the neutral and ion. The FC factors for the ionizations $\chi_n(v = 0) \rightarrow \chi_+(v' = 0, 1, 2...)$ are equal to those of the electron-capture processes where $\chi_+(v' = 0) \rightarrow \chi_n(v = 0, 1, 2...)$.
(96) Liu, D. K.; Brunschwig, B. S.; Creutz, C.; Sutin, N. *J. Am. Chem. Soc.* **1986**, *108*, 1749.

actions. First, the ion/molecule collision is a chemical activation process which releases additional energy into the available degrees of freedom of the precursor complex. The resulting energy distribution was incorporated in eq 16 and 18 as the function $F(E)$. Through rapid statistical fluctuations of the energy distribution in the hot precursor, the critical modes of the complex can be excited, potentially leading to a larger overall value of k_{el}. The amount of chemical activation energy can be significant for ion/molecule collisions involving large polarizable molecules (e.g., the value of ΔE_{im} for the benzene dimer ion,[97] $(C_6H_6)_2^+$, is −15.06 kcal mol^{-1}).[34b]

As noted earlier, differences in the stabilities of the precursor and successor complexes will result in $\Delta E_{PS} \neq \Delta E°$. Therefore, the adiabatic ionization potentials cannot necessarily be used to discuss the energetics and FC factors of the precursor to successor transition. Finally, the structural and electronic properties of the precursor and successor complexes may not be approximated adequately by those of the separated reactants as significant distortions may occur in the collisional complexes.

Correlating Gas-Phase and Solution Reactions. The theoretical connection between the gas-phase reactions and their solution counterparts will be considered here. Similar relationships for other ion/molecule reaction types have been discussed.[52,53] Considering first the formation of the precursor complex, the stability seen in the gas phase, ΔE_{im}^{P} (Figure 2), generally will not be found for solutions due to compensation of attractive ion/molecule forces by desolvation of the ion and, to a lesser degree, of the molecule. However, in solvents with no dipole moment and low polarizabilities an appreciable stability might be found for some ion–neutral combinations in solution. In contrast to the low-pressure gas-phase situation, a solvated precursor complex can be assumed to be thermalized. The formation of the activated complex for electron transfer then requires nuclear fluctuations of the molecules and solvent subsystems, as first described by Marcus.[37,38] From an alternate point of view, the solvation energy of the activated complex (Figure 2) is less than that of the separated reactants and the collision complexes.

Perhaps one of the most intriguing aspects of the gas-phase experiments is the possibility for determination of internal reorganization barriers that can be incorporated in the theoretical description of solvated reactants. Although the contribution of inner reorganization barriers is clearly seen in solution data,[5] no absolute experimental separation of inner and outer barriers has been possible. The experimental and theoretical approaches discussed here suggest that, in principle, this restriction can be overcome, and a more exact description of condensed-phase redox processes may in turn be possible.

Conclusions. For gas-phase electron-transfer reactions with low exoergicities, the estimated intrinsic reorganization barriers appear to correlate with the observed efficiencies. Slow reactions are associated with large changes in bond distances in ion to neutral conversions. Among the metallocenes, inefficient self-exchange and cross reactions are associated with the manganocenes, which have a high-spin/low-spin equilibrium in the neutral form; the rates of the self-exchange reactions decrease for increasing high-spin character.

(97) Field, F. H.; Hamlet, P.; Libby, W. F. *J. Am. Chem. Soc.* **1969**, *91*, 2839.

The simple harmonic oscillator model has been used frequently to predict inverted regions for many condensed-phase bimolecular reactions. We have shown that this model is probably inadequate for discussion of electron-transfer processes involving the metallocenes in the gas phase. This inadequacy arises from the need to include factors which tend to broaden FC manifolds and, potentially, lead to overlap of various ion electronic states. For both gas-phase and condensed-phase electron-transfer processes, care must therefore be taken that the models used to describe the electronic/vibrational properties of the reactant and product states are sufficiently accurate to warrant application of a predictive model for the rates. Future refinements of the theory of electron-transfer reactions will be most successful when sufficient improvements are also made in the relevant theoretical models for the molecular species involved.

Acknowledgment is made to the donors of the Petroleum Research Fund, administered by the American Chemical Society, for partial support of this work (D.E.R.). Additional support was also provided by grants from Research Corp. (D.E.R.) and the Office of Naval Research (J.R.E.). Helpful discussions with P. Kebarle, T. J. Meyer, B. Brunschwig, N. Kestner, and N. Sutin are gratefully acknowledged. We thank C. Walton for expert assistance with synthesis.

Appendix. Rate Expressions

The following is a derivation of the integrated rate expression incorporating the rate of ion loss from the ion trap for irreversible cross reactions. A pseudo-first-order rate constant, k_1, applies for the irreversible reaction (A1). Let k_λ and k_λ' be the first-order

$$A^+ \xrightarrow{k_1} B^+ \tag{A1}$$

rate constants for the loss of ions from the ion trap. At time t, the concentrations of A^+ and B^+ are given by eq A2 and A3

$$[A^+] = [A^+]_0 e^{-(k_1+k_\lambda)t} \tag{A2}$$

$$[B^+] = \left(\frac{k_1[A^+]_0}{k_1 + k_\lambda - k_\lambda'}\right)[e^{-k_\lambda' t} - e^{-(k_1+k_\lambda)t}] \tag{A3}$$

where $[A^+]_0$ is the concentration of A^+ at $t = 0$. The ratio of the concentrations at time t is then

$$R_t = \frac{[A^+]}{[B^+]} = \left(\frac{k_1 + k_\lambda - k_\lambda'}{k_1}\right)\left[\frac{1}{e^{(k_1+k_\lambda-k_\lambda')t} - 1}\right] \tag{A4}$$

Substituting Δk_λ for $k_\lambda - k_\lambda'$ and rearranging eq A4 gives eq A5.

$$\ln\left(\frac{R_t}{R_t + 1}\right) = \ln(k_1 + \Delta k_\lambda) - \ln[k_1 e^{(k_1+\Delta k_\lambda)t} + \Delta k_\lambda] \tag{A5}$$

In the limit where $\Delta k_\lambda \ll k_1$, eq A5 reduces to eq 2 since $k_1 = k_f P$.

Registry No. Cp_2Cr^+, 12793-15-6; Cp_2Mn^+, 73138-26-8; Cp_2Fe^+, 12125-80-3; Cp_2Co^+, 12241-42-8; Cp_2Ni^+, 11091-00-2; Cp_2Ru^+, 54538-51-1; $(Me_5Cp)_2Mn^+$, 71163-80-9; $(MeCp)_2Mn$, 32985-17-4; $Cr(CO)_6^+$, 54404-20-5; Cp_2Co, 1277-43-6; Cp_2Cr, 1271-24-5; Cp_2Ni, 1271-28-9; Cp_2Fe, 102-54-5; Cp_2Mn, 73138-26-8; Cp_2Ru, 67506-86-9; $(Me_5Cp)_2Mn$, 74507-62-3; $(Me_5Cp)_2Co$, 1287-13-4; $Cr(CO)_6$, 13007-92-6; SF_6^-, 25031-39-4; SF_6, 2551-62-4.